School of Pharmacy[1], Wannan Medicinal College; Provincial Engineering Laboratory for Screening and Reevaluation of Active Compounds of Herbal Medicines in Southern Anhui[2]; Anhui Innovative Center for Drug Basic Research of Metabolic Diseases[3],Wannan Medical College, Wuhu; School of Pharmacy[4], Anhui University of Chinese Medicine; Synergetic Innovation Center of Anhui Authentic Chinese Medicine Quality Improvement[5]; Anhui Province Key Laboratory of Chinese Medicinal Formula[6], Hefei, China

An anti-inflammatory active ingredients in *Poriae cutis*: Screening based on network pharmacology

Runze Jin[1], Zitong Zhao[1], Qing Zhang[1], Yu Sun[1,2,3], Wei Wang[1], Daiyin Peng[4,5,6,*], Sihui Nian[1,2,3,*], Lingyun Zhou[1,2,3,*]

Received October 25, 2023, accepted November 27, 2023

**Corresponding authors: Daiyin Peng, Sihui Nian, Ling-yun Zhou, School of Pharmacy, Wannan Medicinal College, 22 Wenchang Western Road, Wuhu 241002, People's Republic of China*
zly-1234@sohu.com

Pharmazie 79: 72-81 (2024) *doi: 10.1691/ph.2024.3647*

Hyperuricemia (HUA) is a disorder of uric acid metabolism, which can lead to the formation of gouty arthritis, kidney inflammation and other damages. Previous studies have found that the alcohol extract of *Poria cutis* can reduce the level of uric acid and protect against kidney injury. Based on network pharmacology, the core targets and main active components of *P. cutis* intervention in HUA were determined. Most of the potential active ingredients are triterpenoid acids such as tumulosic acid (TA) and eburicoic acid (EA), and the potential targets are TNF and IL-6, which are associated with inflammation. *In vitro* experiments have shown that TA can significantly inhibit the release of NO, TNF-α and IL-6 in inflammatory RAW264.7 cell culture medium and the expression of TNF-α and IL-6 in RAW264.7 cells. This study suggests that TA based on network pharmacological screening has obvious anti-inflammatory effect on inflammatory RAW264.7 cells and is a promising anti-inflammatory compound.

1. Introduction

Hyperuricemia (HUA) is a highly prevalent chronic metabolic disease caused by purine metabolism disorders, which is mainly related to high serum uric acid level, and the excretion of uric acid will increase the burden on the kidney, resulting in kidney inflammation and other damage. Improvement of hyperuricemia has been reported to be associated with reduced kidney inflammation and renal fibrosis (Wang et al. 2013). In our previous study, it was found that the ethanol extract of *P. cutis* lowers uric acid contributes to renal protection (Zhao et al. 2023). Therefore, hyperuricemia was selected and the effective components of *P. cutis* were screened by network pharmacology.

Poria cocos is a commonly used medicinal and edible homologous plant, which indicates that its use is relatively safe. *Poria cocos* can be divided into *Poria cocos* and *P. cutis* according to different medicinal parts (Deng et al. 2020), and the triterpenoids and polysaccharides contained have a wide range of pharmacological activities, such as diuretic, anti-inflammatory, antioxidant and other biological activities (Cui et al. 2019; Zhang et al. 2021). The active ingredients and important targets of *P. cutis* in treating HUA were screened through network pharmacology. Triterpenoids were the main monomer components reported in ethanol extracts. Based on network pharmacology, we can quickly screen out the substances with high activity and potential targets. The screened monomers were further verified by cell experiments *in vitro*. In this study, the top ingredients selected by network pharmacology were tumulosic acid (TA) and eburicoic acid (EA). EA has been reported in detail to have *in vitro* anti-inflammatory effect on inflammatory RAW264.7 (Wang et al. 2017), while the NO release of TA was only preliminarily described (Supinya et al. 2008). Therefore, TA was added to evaluate the release of TNF-α and IL-6 in the supernatant of inflammatory RAW264.7 cell culture and the expression levels of TNF-α and IL-6 mRNA in cells. This paper provides a rapid method to search for effective components and potential targets from *P. cutis*, which could provide a theoretical basis for finding a more effective treatment for HUA and inflammation-related diseases.

2. Investigations and results

2.1. Prediction results of P. cutis active ingredient target

A total of 72 chemical components related to *P. cutis* were found to be described in the literature (Wang et al. 2019; Fang et al. 2019; Dong et al. 2015). After screening, a total of 20 components met the requirements, as shown in Table 1. The active components of *P. cutis* were mainly triterpenoid acids. In total, 1208 targets of related components were obtained after screening, and all duplicated targets were deleted.

2.2. Acquisition of relevant targets for P. cutis intervention in HUA

A number of 673 targets of *P. cutis* were obtained by combining GEENCARDS, DRUGBANK and OMIM databases, and 289 targets of active ingredients in *P. cutis* were intersected with 673 targets of HUA. Received 33 common targets through microscopic letter platform (http://www.bioinformatics.com.cn/) draw the VENN diagram (Fig. 1).

2.3. PPI network construction

The PPI network was obtained on STRIING 11.5, and then the target protein PPI network was constructed again using Cytoscape 3.9.1. It can be seen that a total of 33 nodes and 99 interaction connections were obtained (Fig. 2). The top 10 targets in degree value were IL-6, TNF, ESR1, PPARG, HSP90AA1, BCL2L1,

Table 1 Information of 20 active ingredients in *P. cutis*

Number	Compound	Structural formula
FLP1	Pachymic acid	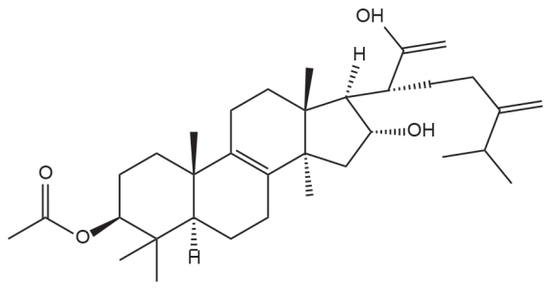
FLP2	Poricoic acid A	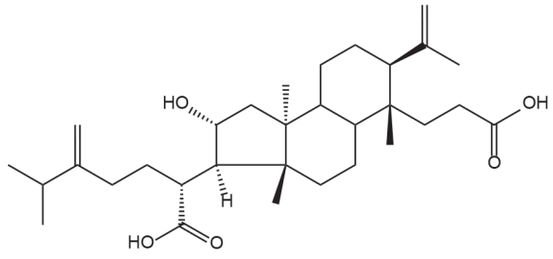
FLP3	Poricoic acid AE	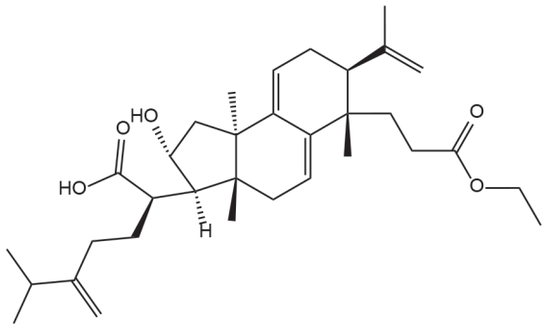
FLP4	Poricoic acid B	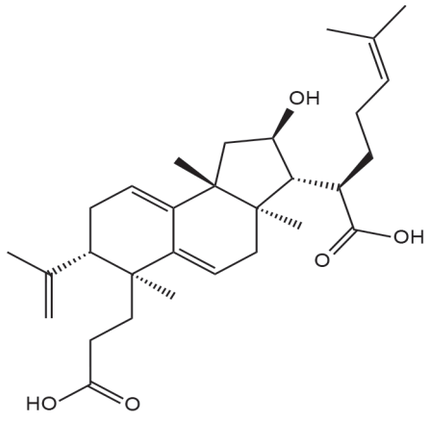
FLP5	Dehydropachymic acid	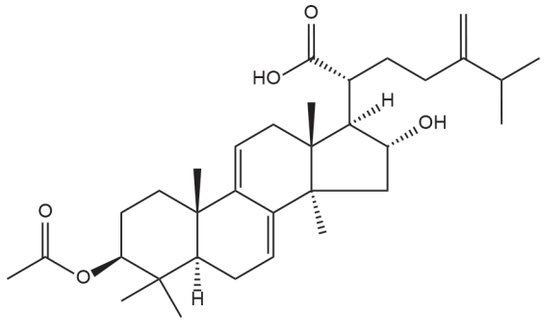

FLP6 3-Epidehydropachymic acid

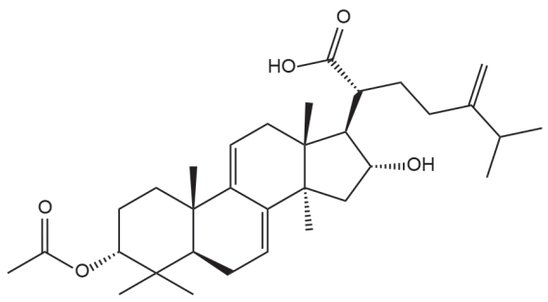

FLP7 Tumulosic acid

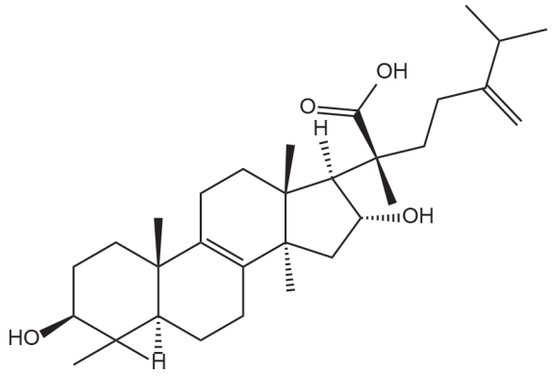

FLP8 Trametenolic acid

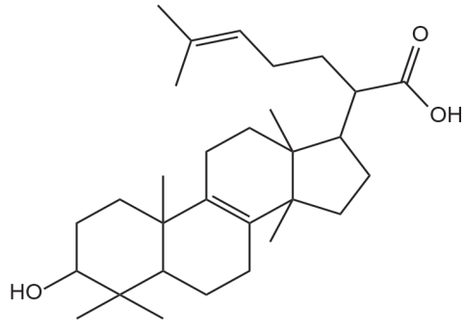

FLP9 Eburicoic acid

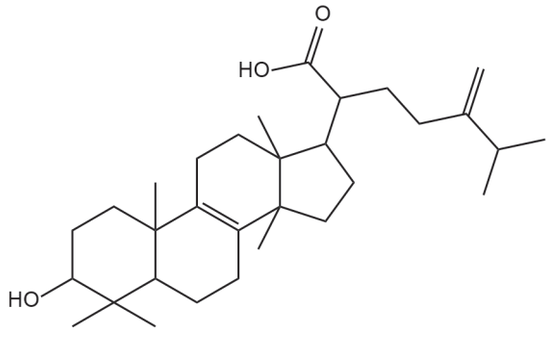

FLP10 3-O-Acetyl-16 alpha-hydroxytrametenolic acid

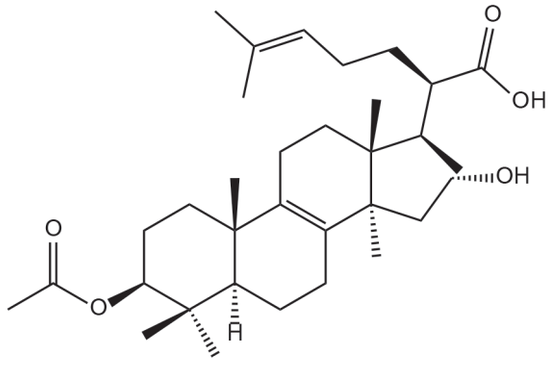

FLP11 16α-Hydroxydehydrotrametenolic Acid

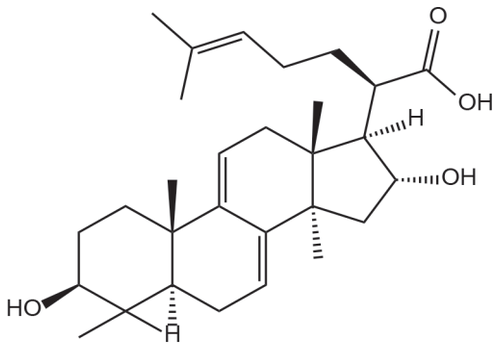

FLP12 Dehydrotumulosic acid

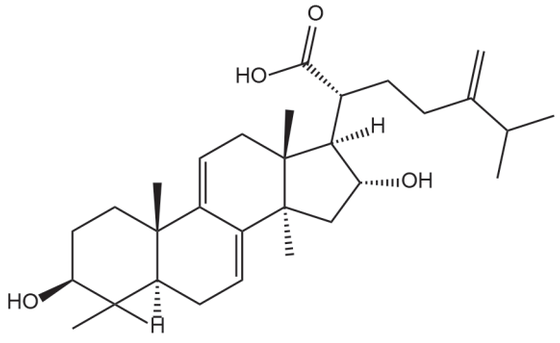

FLP13 Dehydroeburicoic acid

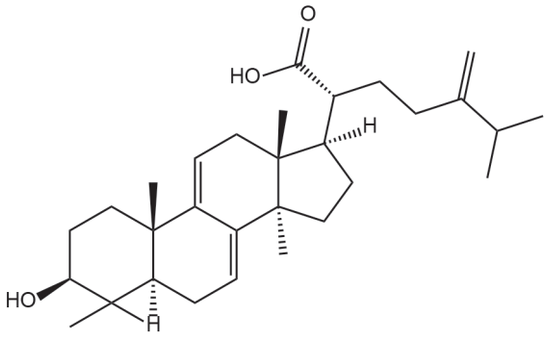

FLP14 Poricoic acid G

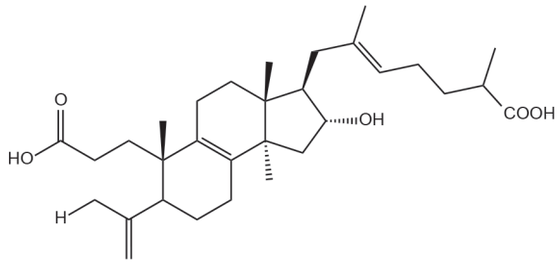

FLP15 Dehydroabietinol

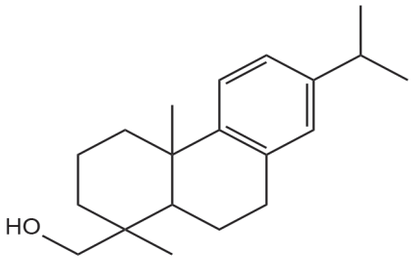

FLP16 Dehydroabietic acid

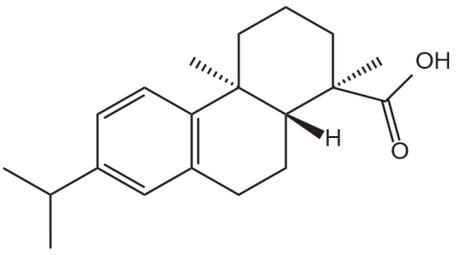

FLP17 Wogonin

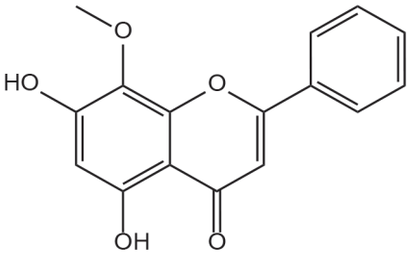

FLP18 3‘,5,6,7,8-Pentamethoxyflavone

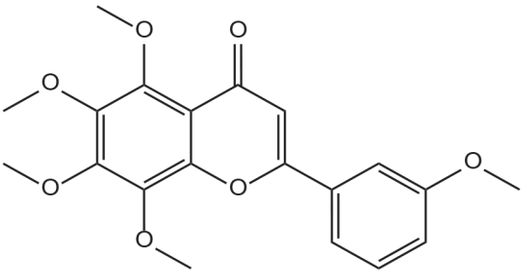

FLP19 4’,7-dihydroxy isoflavone

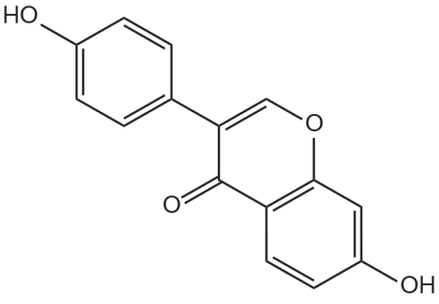

FLP20 Matairesinol

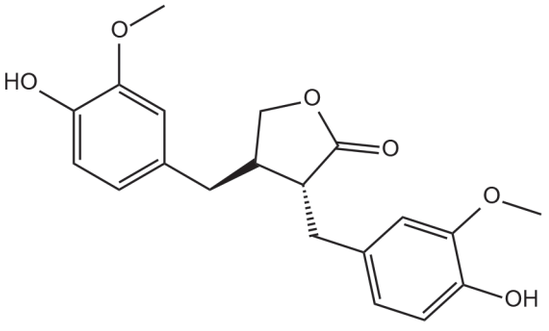

ABCG2, and CYP2C19, indicating that *P. cutis* might exert its therapeutic effect by acting on the above core targets.

2.4. GO annotation and KEGG analysis of key targets

P. cutis interfered with the GO and KEGG enrichment of HUA targets by Metascape analysis. In the GO analysis, a total of 424 biological functions were obtained, and 364 biological processes accounted for a relatively large number of items, mainly involving biological processes such as response to hormones, regulation of defense response, regulation of hormone levels, inflammatory response, regulation of epithelial apoptosis, response to steroid hormones, regulation and negative regulation of lipid storage, and negative regulation of lipid localization. There were 31 cell components, mainly related to neuron cell body, cell body, membrane raft, membrane microdomain, axon, presynaptic, fovea, presynaptic membrane, etc. 29 molecular functions, mainly involving DNA binding TF binding, GPCRs activity, CA binding, nuclear receptor activity, nuclear receptor binding, etc. Figure 3 shows the bar chart of GO entries. Figure 4 shows the visual analysis of

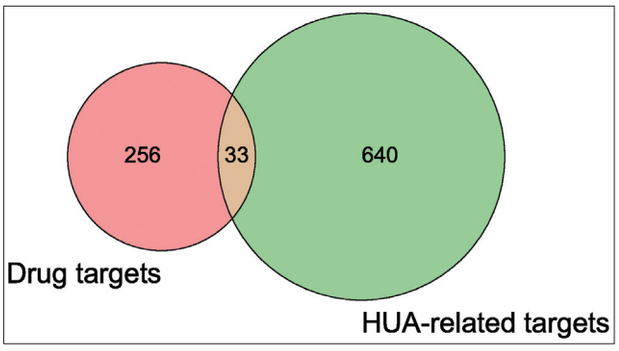

Fig. 1: VEEN diagram of the common target of *P. cutis* and HUA.

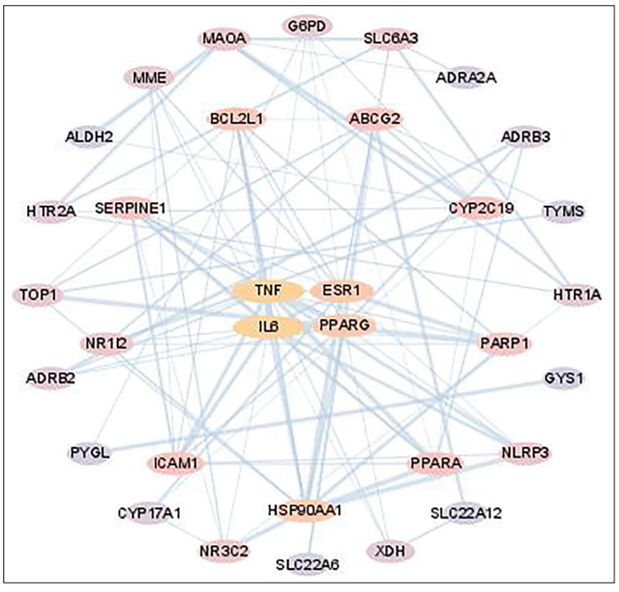

Fig. 2: PPI network of *P. cutis* treating HUA targets.

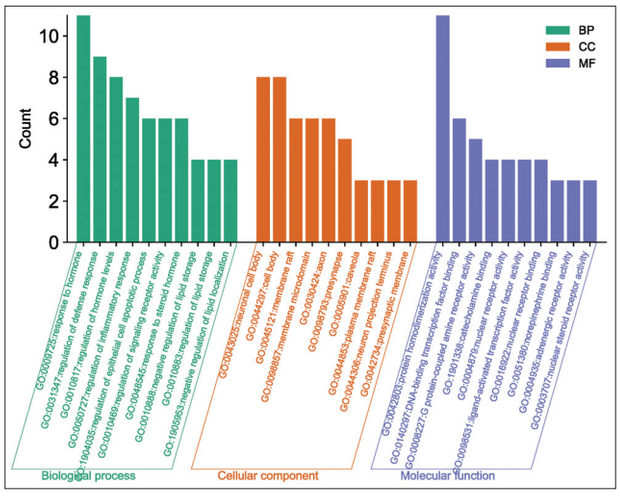

Fig. 3: GO entry analysis of potential targets for *P. cutis* to treat HUA.

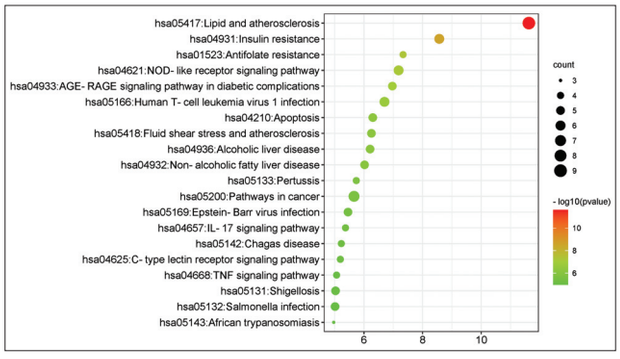

Fig. 4: Enrichment analysis of KEGG pathway in *P. cutis* treatment of HUA.

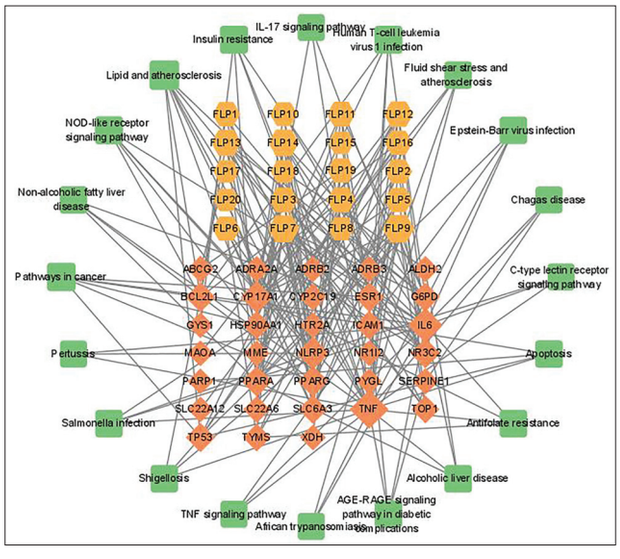

Fig. 5: Composition – target – pathway diagram of *P. cutis* intervention in HUA.

the KEGG pathway. The targets of *P. cutis* were concentrated in cancer, cell death, IL-17 signal, tumor necrosis factor signal and other pathways, indicating that these classical pathways might play an important role in the treatment of *P. cutis* in HUA.

2.5. P. cutis component-target-pathway network construction

CytoScape3.9.1 was used to construct the *P. cutis* component-target-pathway network diagram to analyze the main components and targets of *P. cutis*' intervention in HUA's target parameters, as shown in Fig. 5. The network consisted of 73 nodes and 190 edges, and nodes of different categories were represented by different colors. The area size of the node represented its influence on HUA. In Cytoscape network analysis, each active chemical component and target were cross-connected, which reflected a variety of chemical components contained in *P. cutis*, which might interfere with HUA through multiple targets. The FLP-9 (EA) degree value was 12, the compactness was 0.459, and the mediality was 0.127. EA was predicted to be the main component of *P. cutis* intervention in HUA, followed by FLP-7 (TA) (the connection degree was 11, EA was predicted to be the main component of *P. cutis* intervention in HUA, compactness to 0.426, mediacity to 0.079), FLP-14 (Poricoic G) (connectivity 10, compactness 0.416, mediacity 0.045) (Table 3). The top network node degree targets were TNF, IL6, NLRP3, CYP17A1, PPARG, PPARA, and the connectivity degrees were 26, 18, 14, 13, and 10, which predicted that TNF and IL6 were the core targets of *P. cutis* intervention in HUA. NLRP3, CYP17A1, PPARG, and PPARA were also important (Table 3). In addition, it can be seen from Table 5 that these pathways are not independently separated, but are connected through common targets, which indicates that *P. cutis* plays a synergistic role in the intervention of HUA through multiple pathways.

Table 2: Node characteristics of the main active chemical components of *P. cutis* network

Name	Degree	Closeness Centrality	Betweenness Centrality
FLP9	12	0.458599	0.126417
FLP7	11	0.426036	0.078702
FLP14	10	0.416185	0.045202
FLP13	9	0.436364	0.05486
FLP12	8	0.431138	0.066989
FLP3	6	0.31441	0.042631
FLP4	6	0.31441	0.042631
FLP11	6	0.421053	0.029999

Table 3: Node characteristic parameters of the target network of the main active chemical constituents of *P. cutis*

Name	Degree	Closeness	Betweenness
TNF	26	0.493151	0.34216
IL6	18	0.423529	0.116512
NLRP3	14	0.367347	0.106677
CYP17A1	13	0.382979	0.099264
PPARG	10	0.371134	0.025722
PPARA	10	0.375	0.048227
NR3C2	9	0.352941176	0.023106
BCL2L1	9	0.352941176	0.036197
ESR1	8	0.378947368	0.142222

2.6. Effects of TA and colchicine on cell viability of RAW264.7 cells

Colchicine, a commonly used drug for gouty arthritis, was used as a positive control. Before studying the anti-inflammatory activity of TA, the cytotoxicity of TA and colchicine on RAW264.7 cells were examined by MTT assay method. The cell viability rate was only 45.42% when 2 ug/mL of colchicine was used, while the viability rate of colchicine with a concentration of 1 ug/mL reached 78.67%, so the concentration of colchicine as the positive control was set to 1 ug/mL. As shown in Fig. 6, when RAW264.7 cells were exposed to TA at 60 μg/mL for 24 h, no cytotoxicity was observed in the presence or absence of lipopolysaccharide. However, at higher concentrations (80 and 100 μg/mL), TA could significantly cause cytotoxicity, manifested as decreased cell viability. Therefore, TA concentrations of 20 to 60 μg/mL were chosen for subsequent experiments.

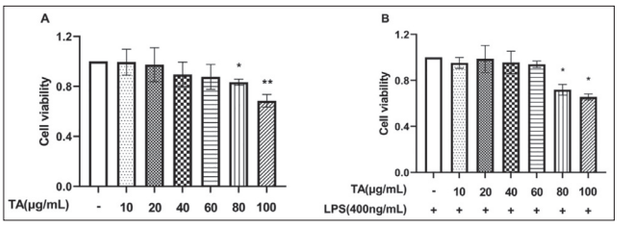

Fig. 6: The effect of different concentrations of TA on cell viability of RAW264.7 cells. A The effect of TA on cell viability when cells were treated with TA alone for 24h. B The effect of co-treatment of TA and LPS for 24h on cell viability. Data are shown as the mean ± SD (n = 5). $^{*}P < 0.05$, $^{**}P < 0.01$ compared with the control or control + LPS group.

2.7. Effect of TA on the release of NO, TNF-α and IL-6 in the supernatant of RAW264.7 cells induced by LPS

According to the results based on network pharmacology, the anti-gout effect of *P. cutis* was related to the expression of two inflammatory cytokines of TNF-α and IL-6, which was also inseparable from the release of NO. Therefore, whether TA affected NO release in LPS-induced RAW264.7 cells was investigated firstly. As shown in Fig. 7(A), RAW 264.7 cells could produce 42.22±1.51 μM NO (measured in nitrite) without any treatment. After adding

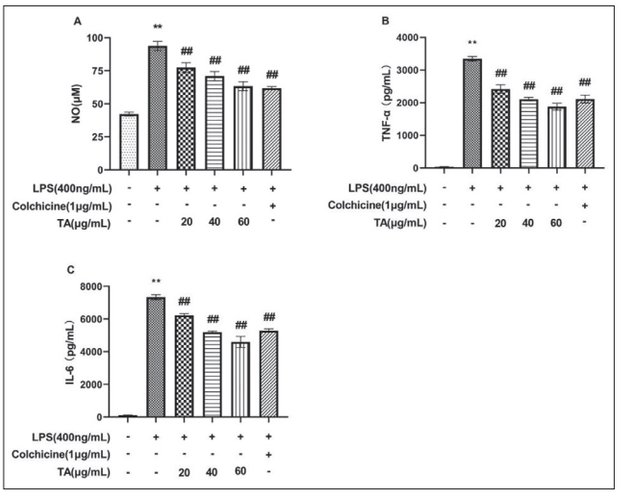

Fig. 7: The effect of different concentrations of TA and colchicine on the release of NO (A), TNF-α (B) and IL-6 (C) in the supernatant of RAW264.7 cells induced by LPS. Compared with the blank group, $^{*}P < 0.05$, $^{**}P < 0.01$; compared with the model group, $^{\#}P < 0.05$, $^{\#\#}P < 0.01$.

Table 4: Enrichment results of *P. cutis*' intervention in HUA target pathway

Go	Description	Count	Gene symbol
hsa05417	Lipid and atherosclerosis	9	BCL2L1,HSP90AA1,ICAM1,IL6,PPARG,TNF,NLRP3
hsa05200	Pathways in cancer	7	BCL2L1,ESR1,HSP90AA1,IL6,PPARG
hsa04931	Insulin resistance	6	GYS1,IL6,PPARA,PYGL,TNF
hsa04621	NOD-like receptor signaling pathway	6	BCL2L1,HSP90AA1,IL6,TNF,NLRP3
hsa05166	Human T-cell leukemia virus 1 infection	6	BCL2L1,ICAM1,IL6,TNF
hsa04933	AGE-RAGE signaling pathway in diabetic complication	5	SERPINE1,IL6,TNF,ICAM1
hsa04210	Apoptosis	5	PARP1,BCL2L1,TNF
hsa05418	Fluid shear stress and atherosclerosis	5	HSP90AA1,ICAM1,TNF
hsa04936	Alcoholic liver disease	5	ALDH2,IL6,PPARA,TNF
hsa04932	Non-alcoholic fatty liver disease	5	IL6,PPARA,PPARG,TNF

400 ng/mL of LPS, NO release was significantly increased to 93.76±3.45 μM ($P < 0.01$). 1 h prior to LPS stimulation, the treatment of cells with 20–60 μg/mL TA could reduce NO release to varying degrees. When the concentration of TA was 60 μg/mL, the inhibitory activity was the strongest, which the NO release amount was 63.33±3.41 μM ($P < 0.01$). Furthermore, we examined the secreted level and mRNA and protein expressions of TNF-α and IL-6. Compared with the normal group, LPS could induce the release of TNF-α from 41.41±6.49 pg/mL to 3344.10±73.43 pg/mL ($P < 0.01$), and the release of IL-6 from 108.33±29.10 pg/mL to 7336.67±162.29 pg/mL ($P< 0.01$). Moreover, pretreatment with TA at 20, 40, 60 μg/mL could significantly inhibit the release of TNF-α and IL-6, compared with those of the LPS-induced group. Among them, TA with a concentration of 60 μg/mL had the strongest inhibitory effect, reducing TNF-α and IL-6 to 1880.51±57.32 pg/mL ($P < 0.01$) and 4597.41±346.36 pg/mL ($P < 0.01$), respectively. Different concentrations of TA inhibited the secreted levels of TNF-α, IL-6 in dose-dependent manners, and the inhibitory effect was comparable to that of the positive control colchicine (1 μg/mL).

2.8. Effect of TA on expression of TNF-α and IL-6 mRNA in RAW 264.7 cells

After determination, the A_{260}/A_{280} of RNA in each group was within the limit of 1.8–2.1, that is, the quality of extracted RNA was qualified. On this basis, the obtained results can be seen: Compared with control cells (1.00±0.11), LPS stimulation increased the mRNA level of TNF-α in RAW264.7 macrophages (47.39±1.86, $P < 0.05$). However, treatment with TA reduced significantly the increase of the mRNA level in a concentration-dependent manner (Figure 8-A). Similarly, LPS also increased the mRNA level of IL-6 compared to the control cell (82.87 ± 5.24, $P < 0.05$), while TA treatment significantly decreased the IL-6 gene expression in a concentration- dependent manner (Figure 8-B).

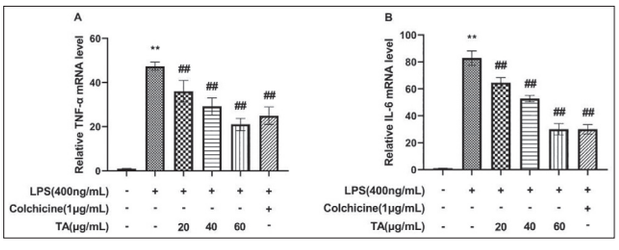

Fig. 8. Effects of TA and colutin at different concentrations on the expression of TNF-αmRNA (A) and IL-6 mRNA(B) in RAW264.7 cells induced by LPS. Compared with blank group, *P < 0.05, **P < 0.01; Compared with the model group, #P < 0.05, ##P < 0.01.

3. Discussion

When HUA occurs, uric acid will be deposited in joints, synovium and other places, further causing inflammation. The occurrence of inflammatory response is triggered by the activation of macrophages, resulting in irreversible damage (Sun et al. 2021). Triterpenoid acid is the principal chemical composition type of *P. cutis*. Many triterpenoid acids can inhibit the expression of COX-2 and iNOS by down-regulating NF-kB (Seulah et al. 2017), play an antioxidant role by scavenging H_2O_2, $\cdot O^{2-}$ and ·OH (Cheng et al. 2011), reduce the reabsorption of electrolytes and water by the kidney and play a diuretic role by competing with aldosterone receptors on the renal surface cells (Akihisa et al. 2007; Zheng et al. 2008). In this study, 289 potential action targets of 20 active ingredients of *P. cutis* were discovered by network pharmacology, and 673 targets related to HUA disease, among which 33 targets of *P. cutis* active ingredients interfered with HUA. According to the results of GO enrichment analysis, the biological processes of *P. cutis* intervention in HUA were mainly hormone regulation, inflammation regulation, DNA binding transcription factor binding, and so on. KEGG's analysis showed that *P. cutis* modulated the cancer pathway, AGE-RAGE signaling pathway, cell death pathway, TNF and IL-17 pathway. Renal diseases can be caused by HUA (Zhao et al. 2022). It can produce various toxic mediators, such as pro-inflammatory cytokines, induce proteinuria, glomerular sclerosis, etc (Thoralf et al. 2003). Studies have found that the activation of AGE receptors and age-RAGE pathway is related to the damage of renal tubules and the aging process, and the occurrence of inflammatory reactions and oxidative stress in different organs and cells are related to the combination of AGE and RAGE (Inagi et al. 2016). Apoptosis pathway can accelerate the occurrence of necrotizing inflammation, HUA and gout can lead to urate deposition in the kidney, resulting in kidney damage, and eventually cause necrotizing inflammation of the kidney (Huang et al. 2023). In the composition-target-pathway network diagram of *P. cutis*, the chemical constituents of *P. cutis* with the highest degree value were mostly triterpenoid acids, such as poric acid and turmoic acid. The key targets of the top 3 with the highest degree value were TNF, IL-6 and NLRP3. In the enrichment analysis of KEGG pathway, TNF and IL-6 correspond to multiple pathways, indicating that the key targets of inflammation were TNF and IL-6. Recent studies have found that inflammatory factors are closely related to HUA and gouty arthritis. IL-6 maintain immune homeostasis and play an important role in the inflammatory response of the body, and it is also one of the key cytokines in acute gouty arthritis (Chen et al. 2020). In the course of the onset of HUA, excessive uric acid increases the burden of the kidney and inflammatory damage, and then a large amount of TNF-α, IL-6, and IL-8 are released (Wang et al. 2022). Studies have shown that HUA and gout are closely related to the levels of inflammatory factors (Lu et al. 2005; Yang et al. 2018; Liu et al. 2014; Cheng et al. 2008). Therefore, the inflammatory response caused by HUA cannot be ignored, and *P. cutis* triterpenoid acids may mainly play their role through inflammatory factor signaling pathways such as TNF and IL-6. Therefore, TA was selected for *in vitro* anti-inflammatory experiments in this study.

The signal transduction process of RAW264.7 activated by LPS is very complex (Smith et al. 2011). The synthesis and release of some important factors and the activation of strong oxidative stress reaction are caused by the activation of mononuclear cells and macrophages by LPS, the initiator of systemic inflammatory reaction, and ultimately lead to cell death and necrosis (Liu et al. 2012). NO is also important in inflammatory response (Zhang et al. 2013). Studies have found that LPS releases a large amount of NO in the process of acute inflammation caused by stimulating RAW264.7 cells (Laroux et al. 2000), and the earliest endogenous mediator in the inflammatory reaction is TNF-α, so it plays a very important role in the inflammatory response (Chang et al. 2016). IL-6 is one of the important factors in immune function regulation and inflammatory response, as well as an important medium for the body's response to tissue infection and injury (Wellby et al. 2001). Therefore, reducing the synthesis or release of NO, TNF-α and IL-6 has important significance in reducing inflammation.

In this research, the acute inflammation model was established by stimulating RAW264.7 cells with LPS. After determining the cell viability and drug dose, the contents of NO, TNF-α and IL-6 in cell fluid with varying TA concentrations were determined, and the expressions of TNF-α and IL-6 were detected by RT-PCR. The results showed that tumulosic had a significant inhibitory effect on the release or secretion of NO, TNF-α and IL-6, which proved that TA may be a potential compound for treating some diseases related to NO, TNF-α and IL-6.

4. Experimental

4.1. Drugs, reagents and instruments

Mononuclear macrophage leukemia cells (mouse) (RAW264.7) were purchased from Procell Life Science&Technology Co., Ltd. Tumulosic acid (Chengdu Push Biotechnology Co., LTD), dimethyl sulfoxide (Beijing Soleibole Technology Co., LTD.), LPS

(Merck Sigma Germany), Trizol lysate, 1510 enzyme marker (Thermo Fischel Technology Co., LTD.), Mouse TNF-α/IL-6 ELISA kit (Wuhan Aibotek Biotechnology Co., LTD.) PCR kit, reverse transcription kit (Biosharp Co., LTD.) colchicine (Xi 'an Virgin Biological Co., LTD.), T100 gradient PCR instrument (Bole Life Medical Products Co., LTD.), StepOne Plus fluorescent quantitative PCR instrument (Singapore Biotechnology Company), JW-3021HR high-speed frozen centrifuge (Anhui Jiaven Instrument Equipment Co., LTD.) were used.

4.2. Screening of candidate components and targets of P. cutis

Information about the chemical components of *P. cutis* were taken from the literature. Their molecular structure diagrams were matched in PubChem database (https://pubchem.ncbi.nlm.nih.gov/) (Dashti et al. 2019), stored in 3Dsdf format, and then uploaded to the Swiss ADME platform (http://www.swissadme.ch/) (Sympli et al. 2021). We standardized all of potential core compounds as follows: 1. Gastrointestinal absorption is "High", indicating that the ingredient has good oral bioavailability and can be absorbed. 2. Two or more of the five types of drug property prediction results (Lipinski, Ghose, Veber, Egan, Muegge) with the positive results are accepted. Finally, the compounds excluded according to the screening criteria were further checked through the literature. If the compounds had obvious pharmacological effects related to the research topic, they were further included. SwissTargetPrediction (http://www.swiss targetprediction.ch/) were employed to search the related targets of potential compounds (Daina et al. 2019). Known targets of unpredicted active compounds were also supplemented according to the literature.

4.3. Screening of targets related to hyperuricemia

The protein targets related to hyperuricemia from several databases including the OMIM database (https://omim.org/) (Moulinath et al. 2021), Gene Cards database (https://www. genecards.org) (Luo et al. 2022), DRUGBANK database (https://www.drugbank. ca/) were retrieved. Known targets of active ingredients but not predicted were added to all targets for further investigation (Wishart et al. 2018). Then, disease targets and potential targets of active components were standardized as Gene Symbols in the UniProt (https://www. uniprot.org/) database (Mohamed et al. 2020). Afterwards, the two types of targets were mapped to obtain the potential targets of *P. cutis* for the treatment of hyperuricemia.

4.4. The construction of PPI network based on the components of P. cutis – the target of hyperuricemia

Protein-protein interaction (PPI) referred to the study of the correlation between chemical compounds and disease-related proteins from the perspectives of biochemistry, signal transduction and genetic networks. In order to elucidate the role of the target protein at the system level, the above targets were uploaded to the STRING11.0 database (https://string-db.org) (Szklarczyk et al. 2021). The species was limited to "Homo sapiens", and the confidence level of the target association set to 0.40. The CytoScape3.9.1 software was used to make the network picture for obtaining the PPI network relationship.

4.5. GO function enrichment and KEGG pathway enrichment based on the components of Poria cocos – the targets of hyperuricemia

The common targets of the active ingredients of *P. cutis* and hyperuricemia were input into Metascape (https://metascape.org/gp /index.html#/main/step1) for GO analysis and KEGG analysis (Zhou et al. 2019), where the GO analysis included biological process (BP), cellular component (CC) and molecular function (MF). The species type was set to H. sapiens. The analysis results were sorted according to the P value from small to large, and $P \leq 0.01$ was required. Moreover, the top 10 and top 20 data were selected for GO enrichment and KEGG pathway analysis. The histogram from GO enrichment and the bubble chart from KEGG enrichment analysis were drawn online using the Weishengxin platform (http://www.bioinformatics.com.cn/).

4.6. Network construction and analysis

To comprehensively analyze the potential mechanism of *P. cutis* in the treatment of hyperuricemia, two network diagrams, drug-target-disease diagram and target-biological pathway diagram, were upload to Cytoscape 3.9.1 to construct a drug-target-pathway diagram. The Network Analyzer tool of CytoScape 3.9.1 was used to analyze the network topology parameters of effective components and targets, including degree, betweenness and closeness, etc. (Wang et al., 2020). Futhermore, the core targets and the main active ingredients in the intervention of hyperuricemia were determined.

4.7. Cell culture and treatment

The experimental method was carried out with reference to the literature (Tang et al., 2023). RAW264.7 cells were seeded into DMEM flasks containing 10% fetal bovine serum, 100 U/mL penicillin and 100 U/mL streptomycin at 37 °C in a humidified environment of 5% CO_2 /air. Tumoric acid (TA) was dissolved in DMSO maintained at 0.5% of the entire DMEM medium (v/v), as this concentration was not significantly toxic to these cells. TA was formulated and added to the medium at the set final concentration.

4.8. Cell viability assay

The effect of TA on cell viability was determined by the tetramethylazolium salt colorimetric (MTT) method. After 24 h incubation, the exponentially growing RAW264.7 cells were seeded at 5×10^4 cells/well in a 96-well plate. After culturing for 24 h, different concentrations of TA (20–60 μg/mL) and positive control colchicine were added and treated for 1 h, and then incubated with the absence or presence of lipopolysaccharide (400 ng/mL) for 24 h. After incubation, 50 μL of MTT was added to each well and then incubated for 4 h. The supernatant was carefully removed from each well, and the formazan precipitate was fully dissolved in 150 μL of DMSO by shaking for 15 min. The absorbance of the samples was detected with a Microplate Reader at 570 nm. Cell viability was calculated as follows: % cell survival = (OD of the experimental group – OD of the blank group) / (OD of the control group – OD of the blank group) × 100.

4.9. Assays of the released levels of NO, TNF-α and IL-6 in the culture supernatant

The experimental method was carried out with reference to the literature (Sun et al.,2020; Wang et al., 2021). RAW264.7 cells were seeded into a 6-well plate at a density of 4×10^6 cells/well and cultured overnight. Cells were treated with different concentrations of TA and 1 μg/mL of colchicine for 1 h, and then treated with LPS (400 ng/mL) for 24 h. The culture medium was centrifuged at 1000 rpm, and the supernatant was collected. The concentration of NO in the culture supernatant was detected according to the nitric oxide detection kit, while the release levels of TNF-α and IL-6 were determined with the corresponding ELISA kit.

4.10. Detection of TNF-α and IL-6 gene expression levels by RT-PCR

The experimental method was carried out with reference to the literature (Wang et al., 2020). RAW264.7 cells were seeded in a 6-well culture plate at a density of 4×10^6 cells/well, treated with turmoic acid and 1 μg/mL of colchicine for 1 h, treated with or without lipopolysaccharide (400 ng/mL), and then incubated for 24 h. Total cellular RNA was extracted with the Trizol Reagent. After the RNA quality test was qualified, reverse transcription was performed with Reverse Transcription Kit (with dsDNase). Real-time quantitative polymerase chain reaction was performed with Universal SYBR qPCR Master kit in a 20 μL reaction system, and quantitative reverse transcription polymerase chain reaction was carried out on Applied Biosystems instrument (software V2.2). PCR amplification included pre-denaturation at 95 °C for 2 min, followed by 40 cycles of denaturating at 95 °C for 15 s and annealing at 60 °C for 30 s. The2-△△CT method was used for the calculation of the relative expression of the target gene. The primer sequences are shown in Table 5.

Table 5: RT-PCR primer sequence

Gene	Forword	Reverse
GAPDH	CATCACCATCTTCCAGGAGCG	GAGGGGCCATCCACAGTCTTC
TNF-α	AGATAGCAAATCGGCTGACG	ACGGCATGGATCTCAAAGAC
IL-6	TACTCGGCAAACCTAGTGCG	GTGTCCCAACATTCATATTGTCAGT

4.11. Statistical analysis

All data were indicated as mean±standard deviation (SD). SPSS Statistic 23.0 software was used for statistical analysis. The statistical significance was analyzed by one-way analysis of variance (ANOVA). LSD was used for multiple comparison test between groups when the variance was uniform, and Dunnett's test was used when the variance was unequal. The difference was considered statistically significant when $P < 0.05$.

Conflicts of interest: There are no financial or other issues that might lead to conflicts of interest.

Funding: The work was supported by Xin 'an Institute of Medicine and Chinese Medicine modernization "open list" project (2023CXMMTCM007), the University Synergy Innovation Program of Anhui Province (GXXT-2019-043) and the Natural science research project of universities in Anhui Province (2023AH040249).

Author Contributions: Funding acquisition, P.D-Y. and N.S-H.; methodology, Z.L-Y., Z.Z-T., J.R-Z., S.Y., W.W. and Z.Q.; resources, Z.Z-T. and J.R-Z.; writing-review and editing, Z.L-Y. and Z.Z-T. All authors have read and agreed to the published version of the manuscript.

Data Availability Statement: All data were obtained from Wannan Medical College and affiliated institutions, and the corresponding author can provide all original content. We declare that no data were derived from third parties, and no paper mill was used.

References

Akihisa T, Nakamura YJ, Tokuda H, Uchiyama E, Suzuki T, Kimura Y, Uchikura K, Nishino H (2007) Triterpene acids from *Poria cocos* and their anti-tumor-promoting effects. J Nat Prod 70: 948–953.

Chang XJ, Fan QR, Wang HM, Zhou J, Li N, Wang ZZ, Xiao W (2016) Effect of Reduning Difang on expression of inflammation-related factors in RAW 264.7 cells. World Sci Technol (TCM Modernization) 18: 286–290.

Chen X, Lu Y, Hua L, Ze K, Yang YY, Wang YF, Zhang M, Li B, Zhou M (2020) Effect of knotweed gout granule on expression of IL-6, TNF-α and PGE_2 in acute gouty arthritis model rats. Chin J Trad Chin Med 35: 3631–3634.

Cheng SH, Li HF, Sun XB, Qin XH, Dai ZQ (2008) Effects of Zangfangmaoru powder on the contents of TNF-α, IL-1 and IL-6 in rats with gouty arthritis induced by sodium urate. J Shanxi Coll Trad Chin Med 9: 13–14.

Cheng SM, Gui Y, Shen S, Huang W (2011) Study on antioxidant activity of triterpenoids from *Poriae cutis*. Food Sci 32: 27–30.

Cui XH, Zhang P, Zhu D (2019) Advances in pharmacological activities of triterpenoids of *Poria Cocos*. Pharmacoeconomics 14: 123–125.

Daina A, Michielin O, Zoete V (2019) Swiss Target Prediction: updated data and new features for efficient prediction of protein targets of small molecules. Nucleic Acids Res 47: W357–W364.

Dashti H, Wedell JR, Westler WM, Markley J, Eghbalnia HR (2019) Automated evaluation of consistency within the PubChem Compound database. Sci Data 6: 190023.

Deng TM, Peng DY, Yu NJ, Wang L, Zhang Y, Ding ZX, Cheng Y, Chen WD, Liu CX (2020) Research progress of chemical constituents and pharmacological effects of *Poria Cocos* and predictive analysis of quality markers. J Chin Herb Med 51: 2703–2717.

Dong JH (2015) Study on chemical constituents and antitumor activity of triterpene extract of *Poriae cutis*. China Academy of Chinese Medical Sciences.

Fang X, Ding XP, Zan JF, Li H, Zhu Y, Dai L, Liu JF (2019) Research progress on chemical constituents and pharmacological effects of *Poriae cutis*. Asia-Pac Trad Med 15: 187–191.

Huang YF, Yin YZ, Shao ZL, Zhang WP, Hu RX, Tong Y (2023) To investigate the effect of Pachymaria plantaginae on uric acid nephropathy based on network pharmacology and molecular docking. J Chin Med Libr Inf 47: 21–26.

Inagi R (2016) RAGE and glyoxalase in kidney disease. Glycoconjugate J 33: 619–626.

Laroux FS, Lefer DJ, Kawachi S, Scalia R, Cockrell AS, Gray L, Van der Heyde H (2000) Role of nitric oxide in the regulation of acute and chronic inflammation. Antiox Redox Signal 2: 391–396.

Lee S, Lee D, Lee SO, Ryu JY, Choi SZ, Kang KS, Kim KH (2017) Anti-inflammatory activity of the sclerotia of edible fungus, Poria cocos Wolf and their active lanostane triterpenoids. J Funct Food 32: 27–36

Liu CL, Cheng L, Ko CH, Wong CW, Cheng WH, Cheung DW, Leung PC, Fung KP, Lau CB (2012) Bioassay-guided isolation of anti-inflammatory components from the root of *Rehmannia glutinosa* and its underlying mechanism via inhibition of iNOS pathway. J Ethnopharmacol 143: 867–875.

Liu ZF, Ma HX, Li XN, Lu T, Wang LH, Wang CX (2014) Comparison of inflammatory cytokines levels between gouty arthritis and hyperuricemia. Trad Chin Med Western Chin 27: 157–158.

Lu W (2005) Study on the relationship between serum uric acid, TNF-α and IL-6 in primary hyperuricemia. Qingdao University.

Luo Y, Fu Y, Tan TF, Hu J, Li F, Liao ZC, Peng J (2022) Screening of lncRNA-miRNA-mRNA coexpression regulatory networks involved in acute traumatic coagulation dysfunction based on CTD, GeneCards, and PharmGKB databases. Oxid Med Cell Longevity 2022: 7280312.

Moulinath A, Priyanka P (2015) Disease-phenotype deconvolution in genetic eye diseases using Online Mendelian Inheritance in Man (OMIM) database. Invest Ophthalmol Vis Sci 56: 1262.

Smith PD, Smythies LE, Shen R, Greenwell-Wild T, Gliozzi M, Wahl SM (2011) Intestinal macrophages and response to microbial encroachment. Mucosal Immunol 4: 31–42.

Soudy M, Anwar AM, Ahmed EA, Osama A, Ezzeldin S, Mahgoub S, Magdeldin S (2020) UniprotR: Retrieving and visualizing protein sequence and functional information from Universal Protein Resource (UniProt knowledgebase). J Proteomics 213: 103613.

Sun L (2021) Study on mechanism of action of Tongfengding capsule in the treatment of gout and hyperuricemia based on network pharmacology. Dali University.

Sun SP, Li SL, Du YY, Wu CG, Zhang MY, Li JR, Zhang XP (2020) Anti-inflammatory effects of the root, stem and leaf extracts of Chloranthus serratus on adjuvant-induced arthritis in rats. Pharm Biol 58: 528-537.

Sympli HD (2021) Estimation of drug-likeness properties of GC-MS separated bioactive compounds in rare medicinal *Pleione maculata* using molecular docking technique and SwissADME in silico tools. Netw Model Anal Health Inform Bioinform 10: 14.

Szklarczyk D, Gable AL, Nastou KC, Lyon D, Kirsch R, Pyysalo S, Doncheva NT, Legeay M, Fang T, Bork P, Jensen LJ, von Mering C (2021) Correction to 'The STRING database in 2021: customizable protein-protein networks, and functional characterization of user-uploaded gene/measurement sets. Nucl Acids Res 49: 10800.

Tang ZY, Zhang MR, Gao L, Bao YL, Li P, Wang M, Shao TL,Wang GD, Liu CY (2023) Optimal extraction of polysaccharides from Stevia rebaudiana roots for protection against hydrogen peroxide-induced oxidative damage in RAW264.7 cells. Nat Pro Res 37:1-5

Tewtrakul S, Wattanapiromsakul C, Mahabusarakam W (2008) Effects of compounds from *Garcinia mangostana* on inflammatory mediators in RAW264.7 macrophage cells. J Ethnopharmacol 121: 379–382.

Wang BJ, Xie PF, Guo XY, Zhou H, Hu H, Wang Y, Qiao Y, Wang XL, Wang CH, Hu Y (2022) Effect of Qingre Xiezhuo prescription combined with benzbromarone on the treatment of asymptomatic HUA dampness-heat syndrome and serum inflammatory factors. World J Integr Med 17: 1788–1791.

Wang J, Li D, Ni W, Qin XJ, Liu H, Wang J, Li D, Ni W, Qin XJ, Liu H, Yu LL, Qiao X, Ji YH, He L, Nian SH, Liu HY (2020) Molecular networking uncovers steroidal saponins of Paris tengchongensis. Fitoterapia 145:104629.

Wang JZ, Zhang P, He HB, Se XX, Sun WJ, Chen BY, Zhang L, Yan XM, Zou K (2017) Eburicoic acid from *Laetiporus sulphureus* (Bull.:Fr.) Murrill attenuates inflammatory responses through inhibiting LPS-induced activation of PI3K/Akt/mTOR/NF-κB pathways in RAW264.7 cells. Naunyn-Schmiedebergs Archi Pharmacol 390: 845–856.

Wang L, Wang PP, Wang DD, Tao MQ, Xu WK, Olatunji OJ (2020) Anti-Inflammatory activities of Kukoamine A from the root bark of Lycium chinense Miller. Nat Prod Commun 15: 1-8.

Wang M (2019) Study on the material basis and mechanism of resistance of *Poria* peel to renal fibrosis. Northwestern University.

Wang YZ, Zhang J, Zhao YL, Li T, Shen T, Li JQ, Li WY, Liu HG (2013) Mycology, cultivation, traditional uses, phytochemistry and pharmacology of Wolfiporia cocos (Schwein.) Ryvarden et Gilb.: a review. J Ethnopharmacol 147: 265–276.

Wang ZG, Cheng G, Wu MC (2021) Columbianetin improve Rheumatoid Arthritis and Relative Mechanisms. Lat Am J Pharm 40: 1910-1917.

Wellby ML, Kennedy JA, Pile K, True BS, Barreau P (2001) Serum interleukin-6 and thyroid hormones in rheumatoid arthritis. Metabolism 50: 463–467.

Wendt TM, Tanji N, Guo JC, Kislinger TR, Qu W, Lu Y, Bucciarelli LG, Rong LL, Moser B, Markowitz GS, Stein G, Bierhaus A, Liliensiek B, Arnold B, Nawroth PP, Stern DM, D'Agati VD, Schmidt AM (2003) RAGE drives the development of glomerulosclerosis and implicates podocyte activation in the pathogenesis of diabetic nephropathy. Am J Pathol 162: 1123–1137.

Wishart DS, Feunang YD, Guo AC, Lo EJ, Marcu A, Grant JR, Sajed T, Johnson D, Li C, Sayeeda Z, Assempour N, Iynkkaran I, Liu YF, Maciejewski A, Gale N, Wilson A, Chin L, Cummings R, Le D, Pon A, Knox C, Wilson M (2018) DrugBank 5.0: a major update to the DrugBank database for 2018. Nucl Acids Res 46: D1074–D1082.

Yang YH, Xiao BY, Xie MZ, Hu ZX, Su LJ, Fan FY (2018) Study on correlation between TCM syndrome type of gouty arthritis and IL-1β, IL-6, TNF-α. Chin Trad Med Emerg 27: 625–627.

Zhang CW, ZhangY, Su S, Cheng L (2021) Research progress on the herbology, chemical composition and pharmacological action of *Poria*. Hubei Agricult Sci 60: 9–14.

Zhang M, Wang D, Wan YZ, Ai H, Li JX, Li J (2013) Inhibition of NO production in RAW264.7 cells induced by LPS by daidzein and puerarin. World Sci Technol (TCM Modernization) 15: 648–652.

Zhao FF, Yang XJ (2022) To study the mechanism of Coix Fuzi patrinia powder in the treating hyperuricemia based on network pharmacology. TCM Clin Res 14: 109–115.

Zhao ZT, Nian SH, Sun XQ, Wang W, Zhang Q, Peng DY, Zhou LY (2023) Study on the effect of lowering uric acid and effect on the kidney of Poriae cutis in hyperuricemia mice. J Hainan Med Univ 29: 168–173.

Zheng Y, Yang XW (2008) Two new lanostane triterpenoids from *Poria cocos*. J Asian Mat Prod Res 10: 323–328.

Zhou YY, Zhou B, Pache L, Chang M, Khodabakhshi AH, Tanaseichuk O, Benner C, Chanda SK (2019) Metascape provides a biologist-oriented resource for the analysis of systems-level datasets. Nature Comm 10: 1523.